Proceedings of the 2001 IEEE
International Conference on Robotics & Automation
Seoul, Korea • May 21-26, 2001

# Tactile Differentiator

Makoto Kaneko, Yoshiharu Bessho, Toshio Tsuji

Faculty of Engineering
Hiroshima University
1-4-1 Kagamiyama, Higashi-Hiroshima, Hiroshima 739-8527, JAPAN

## Abstract

*This paper proposes the Tactile Differentiator that can enhance the edge of polygonal surface, through tracing motion. It is composed of a flexible beam anchored at the base with a moment sensor, and an actuator for moving the whole system. When the beam tip passes over the edge where two different planes are intersected with an arbitrary angle, the Tactile Differentiator provides a step change of output, as if it were just like a differentiator. The edge enhancement factor of sensor is introduced with the shape of beam, the intersection angle of environment, and the contact friction. By using the factor, we discuss the design of the sensor. Experimental results are also shown to verify the basic idea.*

**Key words:** *Tactile Differentiator, Whisker Sensor, Edge Detection, Curved Pattern Recognition*

## 1 Introduction

### Background

In automobile companies, many mechanical components are manufactured through molding process. Engine cover, shaft, cylinder, and piston may be good examples where basic forms are first obtained by molding. Those components are, then, sent to various machining process, such as cutting, welding, pressing, lathing, reaming, drilling, and tapping, before assembling them. In assembling line, all components are carefully chosen to assemble an engine with the best combination of components. To make the process easier, a serial number or alphabet mark is often provided on their surfaces after molding, so that we can quickly recognize where the component comes from. The marking process is usually achieved through stamping by dies. This is because the mark never disappears even under oily or dusty environment, with such physical stamping. Fig.1(a) shows an example of mark on a metal plate. For recognizing it, a visual recognition is often introduced in automobile companies since it is the most popular and powerful tool. However, even with a vision, it is impossible to achieve the success rate with 100%, because of the dirt attached on surface during various machining process and perhaps because of the lighting condition. Since each mark is given just like sculpture on the surface, a tactile sensor is surely a good candidate for taking over the recognition procedure when the vision provides with unreliable output.

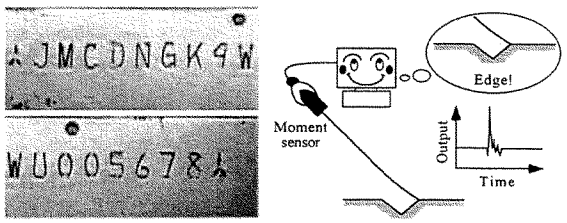


(a) An example of mark given by dies (b) Conceptual image

**Fig. 1**: Conceptual image of Tactile Differentiator

We believe that a high success rate can be achieved by utilizing both vision and tactile information complimentarily. Now, suppose that the vision results in failure in mark recognition. The first step for tactile sensor is to find the edge providing a part of contour of each character. We would note that it is not necessary to fully reconstruct the whole shape where the tactile probe traces but important to know where the edge is. This is because any number or alphabet can be characterized by the edge rather than how the shape of concave looks like. For visual recognition, this step corresponds to the edge enhancement executed by applying an appropriate differentiation process. The second step is the recognition process, where a set of characterized data are compared with the database already stored in the file and find the best matching pattern among them. Actually, the second step is same for both tactile and visual recognition. Knowing of the importance of edge enhancement in the first step, we finally come to the following questions. Can we directly obtain the output enhanced by the edge through a simple tracing motion? If this is the case, how should we design the sensor to match with our request? Within our knowledge, there has been no work addressing this issue while a number of works have tried to obtain the edge information through an appropriate signal processing.

### Goal of this work

The goal of the paper is to propose the sensor system as shown in Fig.1(b), where the edge is enhanced by a simple tracing motion. For simplifying the problem, we consider the environment where a tactile probe traces between two planes whose intersection angle is $\alpha$. Through the paper, we would like to answer the following questions. Under

what sensor configuration, we can find a stepwise change of output when the probe passes over from one to another plane? What parameters are influenced on the sensor output? What sensor configuration is the simplest? Can we confirm the edge enhancement through experiments?

**Main results**
We first derive the relationship between torque sensor output and the displacement of beam tip, when the tip passes over two different planes whose intersection angle is $\alpha$. We introduce the edge enhancement factor of sensor with the shape of beam, the intersection angle of environment, and the contact friction. This factor implies that when the whisker passes over the edge, how much sensor output is amplified. The sensor system whose factor is not equal to unity is termed as Tactile Differentiator. By considering the factor, we design an extremely simple Tactile Differentiator. Finally, through experiments, it is verified that the developed Tactile Differentiator surely provides a step immediately after it passes over the edge.

## 2 Related Works

In general, human touch sensor includes the capability to sense shape recognition, the degree of slip, surface compliance, and temperature. Such touch sensing supplies important sensory information that helps us manipulate and recognize object and warn of harmful situations. So far, a number of artificial tactile sensors have been designed and developed in various research institutes.

**Shape recognition and contact point detection:** Shimojo and others [1] have developed a tactile sheet by utilizing conductive rubber and succeeded in recognizing the object grasped by a multifingered robot hand. Son and Howe [2] have also designed a sophisticated tactile sensor and implemented it into fingertip. Maekawa and others [3] have developed a finger shaped tactile sensor using a hemisphere glass, silicon rubber, light source, and light-electricity conversion devise, for detecting the contact point.

**Slip detection:** For detecting slip, Ueda and others [4] have proposed a sensing mechanism where a slip can be detected through the rotation of a roller supported at the base by spring. Howe and Cutkosky [5] [6] have designed a fingertip covered by rubber with many nibs. When the fingertip makes slip on the contact surface, those nibs pressed due to contact are flipped one by one. The acceleration sensor attached inside the fingertip detects a small acceleration caused by such flipping motion.

**Whisker sensor:** A simple flexible beam sensor can take the form of a short length of spring piano wire or hypodermic tubing anchored at the end. When the free end touches an external object, the wire bends and this can be sensed by a simple switch [7]-[11]. Russel [12] has developed a whisker sensor array and succeeded in reconstructing the shape of convex object followed by the whisker. In our former work [13], we have discussed the basic working principle of tracing type whisker sensor, where we showed that 2-D surface irregularities are observable under a straight-lined whisker with one-axis torque sensor, irrespective of the contact friction.

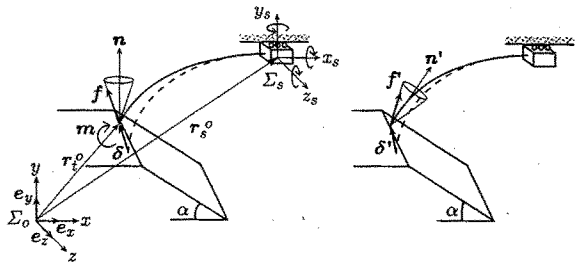

(a) On the horizontal surface (b) On the inclined surface

**Fig. 2**: Coordinate system of whisker sensor

While there have been various works on tactile sensor, at least, we do not know any paper discussing the issue on the edge enhancement through tactile sensing.

## 3 Working Principle

### 3.1 Analytical model

The tactile sensor is composed of a flexible beam anchored at the base with a moment senor and an actuator for moving the whole system, as shown in Fig.2, where $\sum_o$, $\sum_s$, $\boldsymbol{f} = (f_x, f_y, f_z)^t \in R^{3\times1}$, $\boldsymbol{m} = (m_x, m_y, m_z)^t \in R^{3\times1}$, $\boldsymbol{\delta} = (\delta_x, \delta_y, \delta_z)^t \in R^{3\times1}$, $\boldsymbol{n}$, and $\alpha$ denote the world coordinate system, the sensor coordinate system, the contact force, the contact moment, the displacement of the whisker tip due to $\boldsymbol{f}$ and $\boldsymbol{m}$, the normal vector of the contact surface, and the inclination angle with respect to the horizontal plane, respectively. $\boldsymbol{e}_x$, $\boldsymbol{e}_y$, and $\boldsymbol{e}_z$ indicate the unit vectors in each axis in $\sum_o$, respectively. The whisker tip lies on the horizontal surface in Fig.2(a), while it on the inclined surface in Fig.2(b), where "$'$" denotes the parameter on the inclined surface.

### 3.2 Principle behind the idea

The normal direction of contact surface changes suddenly when the tip crosses over an edge, while the tip does not move so much. Since the contact force is bounded by the friction cone whose center axis coincides with the normal direction, it will be necessarily influenced by the step change of normal direction. As a result, the step change of contact force will bring about the similar change for the moment sensor, as well. Of course, the mapping from the change of surface to the sensor output strongly depends upon the shape of whisker. Briefly speaking, this is the basic principle behind the idea. We would emphasize that the step change is not produced by the dynamic vibration but it is expected even under a quasi-static motion.

### 3.3 Assumptions

For simplifying our discussion, we set the following assumptions.
**Assumption 1** : The deformation of whisker is small enough to ensure that we can apply classical beam

theory between the deformation and the contact force (or moment).

**Assumption 2** : The whisker is moving from the horizontal to an inclined plane whose intersection angle is $\alpha$.

**Assumption 3** : The whisker tip always makes contact with the environment to be sensed.

**Assumption 4** : Both static and dynamic friction coefficients are not distinguished each other.

**Assumption 5** : Quasi-static motion is assumed

**Assumption 6** : A moment sensor is implemented into $z_s$-axis

With assumption 2, we can always find the contact force lying on the friction boundary.

### 3.4 Edge enhancement factor :$F$

Now, let us introduce the edge enhancement parameter $F$ for a general whisker model as shown in Fig.2. Assumption 1 guarantees the following linear relationship between force (moment) $\boldsymbol{w} = (\boldsymbol{f}^t, \boldsymbol{m}^t)^t$ and displacement $\boldsymbol{d} = (\boldsymbol{\delta}^t, \boldsymbol{\theta}^t)^t$

$$\boldsymbol{d} = \boldsymbol{D}\boldsymbol{w} \tag{1}$$

$$\boldsymbol{D} = \begin{pmatrix} \boldsymbol{D}_{11} & \boldsymbol{D}_{12} \\ \boldsymbol{D}_{21} & \boldsymbol{D}_{22} \end{pmatrix} \in R^{6\times 6} \tag{2}$$

where $\boldsymbol{\theta} = (\theta_x, \theta_y, \theta_z)^t \in R^{3\times 1}$ and $\boldsymbol{D}_{ij} \in R^{3\times 3}(i = 1,2, j = 1,2)$ denote the angular displacement due to $\boldsymbol{m}$ and the block compliance matrix, respectively. There exists the following relationship between force (moment) at whisker tip and force (moment) $\boldsymbol{w}_s = (\boldsymbol{f}_s^t, \boldsymbol{m}_s^t)^t$ at sensor base.

$$\boldsymbol{w}_s = \boldsymbol{T}\boldsymbol{w} \tag{3}$$

$$\boldsymbol{T} = \begin{pmatrix} \boldsymbol{I}_{3\times 3} & \boldsymbol{O}_{3\times 3} \\ \boldsymbol{T}_1 & \boldsymbol{I}_{3\times 3} \end{pmatrix} \in R^{6\times 6} \tag{4}$$

where $\boldsymbol{I}_{3\times 3} = diag[1,1,1]$, $\boldsymbol{O}_{3\times 3} = diag[0,0,0]$, $\boldsymbol{T}_1 = (\boldsymbol{r}_s^o - \boldsymbol{r}_t^o)\otimes$ and the subscript "$s$" denotes the sensor coordinate system. For $\boldsymbol{r} = (x,y,z)^t$, $\boldsymbol{r}\otimes$ can be expressed by,

$$\boldsymbol{r}\otimes = \begin{pmatrix} 0 & -z & y \\ z & 0 & -x \\ -y & x & 0 \end{pmatrix} \tag{5}$$

For a whisker simply contacting with an environment, we can generally neglect the moment at the whisker tip. Taking this fact into consideration, we focus on the effect caused only by the contact force, which can be written by

$$\boldsymbol{\delta} = \boldsymbol{D}_{11}\boldsymbol{f} \tag{6}$$

While the whisker tip passes over the edge, we can regard that the tip keeps the same height. This constraint condition can be given by

$$\boldsymbol{e}_y^t\boldsymbol{\delta} = \boldsymbol{e}_y^t\boldsymbol{\delta}' \tag{7}$$

where we further assume that the sensor base is moved so that the whisker tip under contact force free may follow along the horizontal line (along $x$-axis).

On the other hand, the contact force can be also expressed in the following form,

$$\boldsymbol{f} = \boldsymbol{R}\begin{pmatrix} f_{t1} \\ f_n \\ f_{t2} \end{pmatrix} \tag{8}$$

$$\boldsymbol{R} = \begin{pmatrix} \cos\alpha & \sin\alpha & 0 \\ -\sin\alpha & \cos\alpha & 0 \\ 0 & 0 & 1 \end{pmatrix} \tag{9}$$

where $f_{t1}$, $f_{t2}$, and $f_n$ are two tangential and normal force components, respectively. For our convenience $t_2$-axis is chosen in such away that it may be parallel to $z$-axis (or $z_s$-axis). Since the contact force always lies on the friction boundary by Assumption 2, we can assign each force component in eq. (8) in the following.

$$\boldsymbol{f} = \boldsymbol{R}\begin{pmatrix} -\mu f_n \\ f_n \\ 0 \end{pmatrix} = f_n\boldsymbol{R}\boldsymbol{a} \tag{10}$$

where $\mu$ is the friction coefficient and $\boldsymbol{a} = [-\mu, 1, 0]^t$. The contact force inevitably changes just after passing over edge, so that it can adapt a new friction constraint. Considering eq.(6) and (10), the constraint condition eq.(7) can be rewritten by

$$f_n\boldsymbol{e}_y^t\boldsymbol{D}_{11}\boldsymbol{R}\boldsymbol{a} = f_n'\boldsymbol{e}_y^t\boldsymbol{D}_{11}\boldsymbol{R}'\boldsymbol{a} \tag{11}$$

Under such a constraint, let us now consider the sensor output coming from the moment sensor around $z_s$-axis. While the sensor with more than one axis, of course, provides us with rich information on surface profile as well as contact force, we are challenging the edge enhancement by a single axis moment sensor alone. This is just because of the minimum sensor realization that generally contributes to developing an economical and robust sensing system. The moment component $m_{zs}$ can be picked up by operating the following selection vector $\boldsymbol{s}_6$ in eq.(3), under $\boldsymbol{m} = 0$

$$\begin{aligned} m_{zs} &= \boldsymbol{s}_6^t\boldsymbol{w}_s \\ &= \boldsymbol{s}_6^t\boldsymbol{T}\boldsymbol{w} \end{aligned} \tag{12}$$

where $\boldsymbol{s}_6 = [0,0,0,0,0,1]^t$. $m_{zs}$ can be also expressed by using $\boldsymbol{f}$.

$$m_{zs} = \boldsymbol{s}_3^t\boldsymbol{T}_1\boldsymbol{f} \tag{13}$$

where $\boldsymbol{s}_3 = [0,0,1]^t$. Replacing $\boldsymbol{f}$ by eq.(10), we finally obtain the following form.

$$m_{zs} = f_n\boldsymbol{s}_3^t\boldsymbol{T}_1\boldsymbol{R}\boldsymbol{a} \tag{14}$$

Under these preparations, we now define the edge enhancement factor in the following.

$$F = \frac{m_{zs}|_{\alpha=\alpha}}{m_{zs}|_{\alpha=0}} = \frac{f_n'\boldsymbol{s}_3^t\boldsymbol{T}_1\boldsymbol{R}'\boldsymbol{a}}{f_n\boldsymbol{s}_3^t\boldsymbol{T}_1\boldsymbol{R}\boldsymbol{a}} \tag{15}$$

Considering the constraint condition eq.(11), eq.(15) can be rewritten by,

$$F = \frac{\boldsymbol{e}_y^t \boldsymbol{D}_{11} \boldsymbol{R} \boldsymbol{a}}{\boldsymbol{e}_y^t \boldsymbol{D}_{11} \boldsymbol{R}' \boldsymbol{a}} \cdot \frac{\boldsymbol{s}_3^t \boldsymbol{T}_1 \boldsymbol{R}' \boldsymbol{a}}{\boldsymbol{s}_3^t \boldsymbol{T}_1 \boldsymbol{R} \boldsymbol{a}} \tag{16}$$

We would note that $F$ is meaningful only under $\boldsymbol{e}_y^t \boldsymbol{D}_{11} \boldsymbol{R}' \boldsymbol{a} \neq 0$ and $\boldsymbol{s}_3^t \boldsymbol{T}_1 \boldsymbol{R}' \boldsymbol{a} \neq 0$. $\boldsymbol{e}_y^t \boldsymbol{D}_{11} \boldsymbol{R}' \boldsymbol{a} = 0$ means that the possible contact force restricted by the friction cone on the inclined surface can not make any $y$-directional displacement at the tip of whisker. On the other hand, under $\boldsymbol{s}_3^t \boldsymbol{T}_1 \boldsymbol{R}' \boldsymbol{a} = 0$, the possible force on the horizontal surface can never produce a moment around the sensor axis. Under $\boldsymbol{e}_y^t \boldsymbol{D}_{11} \boldsymbol{R}' \boldsymbol{a} \neq 0$ and $\boldsymbol{s}_3^t \boldsymbol{T}_1 \boldsymbol{R}' \boldsymbol{a} \neq 0$, $F$ indicates how much jump appears after passing over the edge. The edge enhancement can be expected by $|F|$ with more than unity. We call the whisker sensor whose $|F|$ is more than unity as Tactile Differentiator. For a given test environment, $\boldsymbol{e}_y$, $\boldsymbol{a}$, $\boldsymbol{s}_3$, and $\boldsymbol{R}$ are automatically determined, while $\boldsymbol{a}$ includes an unknown factor $\mu$. Therefore, we can not purposely change these parameters by design. What we can do for the design is to change both $\boldsymbol{D}_{11}$ and $\boldsymbol{T}_1$. Designing $\boldsymbol{D}_{11}$ corresponds to determining a proper whisker shape. On the other hand, designing $\boldsymbol{T}_1$ simply corresponds to determining the height of base for a given whisker. Knowing of the effect on $F$ by each parameter, our goal is to obtain a whisker sensor system with a satisfactory $F$.

## 3.5 Case study: part1

As the first example, we consider the straight-lined whisker, since it has the simplest configuration. For such a whisker, $\boldsymbol{D}_{11}$ and $\boldsymbol{T}_1$ are given as follows.

$$\boldsymbol{D}_{11} = \frac{l^3}{3EI} \begin{pmatrix} s^2 & -sc & 0 \\ -sc & c^2 & 0 \\ 0 & 0 & 1 \end{pmatrix} \tag{17}$$

$$\boldsymbol{T}_1 = l \begin{pmatrix} 0 & 0 & -s \\ 0 & 0 & c \\ s & -c & 0 \end{pmatrix} \tag{18}$$

where $E$, $I$, $l$, $\beta$, $c$ and $s$ are the Young's modulus, the bending moment of inertia, the length of whisker, the setting angle measured from the horizontal plane ($x_s z_s$ plane), $c = \cos\beta$, and $s = \sin\beta$, respectively. Substituting $\boldsymbol{e}_y = (0,1,0)^t$, $\boldsymbol{a} = (-\mu, 1, 0)^t$, $\boldsymbol{s}_3 = (0,0,1)^t$, $\boldsymbol{D}_{11}$, and $\boldsymbol{T}_1$ for eq.(16), we can easily confirm $F = 1$ irrespective of the intersection angle $\alpha$, the setting angle $\beta$, and the friction coefficient $\mu$. In our former work [13], we showed a theorem where a surface profile is observable under a straight-lined whisker with one-axis moment sensor, regardless of contact friction. Such observability of surface profile means that the sensor outputs are same just before and after passing an edge. Therefore, the theorem naturally guarantees $F = 1$ for a straight-lined whisker, irrespective of $\alpha$, $\beta$, and $\mu$. While we can see such a nice coincidence for both approaches, the utilization of a straight-lined whisker is not desirable from the viewpoint of edge enhancement since $F$ is always unity for all possible edges.

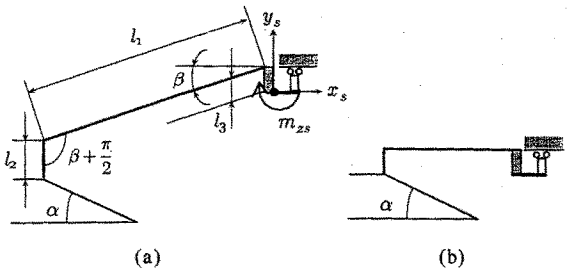


**Fig. 3**: $L$-shaped whisker

## 3.6 Case study: part2

Now, we consider an appropriate whisker whose shape is not much different from the straight one for avoiding complicated form of $F$. The second simplest shape is perhaps an $L$-shaped whisker, as shown in Fig.3(a). Assuming that the elasticity of the sensor comes from the whisker composed of the length of $l_1$ and $l_2$, we can obtain the following components for $\boldsymbol{D}_{11}$ and $\boldsymbol{T}_1$.

$$\boldsymbol{D}_{11} = \frac{l_1^3}{3EI} \boldsymbol{A} \tag{19}$$

$$\boldsymbol{A} = \begin{pmatrix} s^2 + \frac{3}{2}ks + k^3 & -sc - \frac{3}{2}kc & 0 \\ -sc - \frac{3}{2}kc & c^2 & 0 \\ 0 & 0 & (1+k^3) + 3k^2 \frac{EI}{GJ} c^2 \end{pmatrix} \tag{20}$$

$$\boldsymbol{T}_1 = \begin{pmatrix} 0 & 0 & -l_1 s - l_2 + l_3 \\ 0 & 0 & l_1 c \\ l_1 s + l_2 - l_3 & -l_1 c & 0 \end{pmatrix} \tag{21}$$

where $G$, $J$, and $k$ are the modulus of rigidity, the torsional moment of inertia with respect to the center axis of beam, and $k = l_2/l_1$ respectively. Of course, eq.(19) results in eq.(17) under $k = 0$. From eq.(15), we finally obtain $F$ in the following form.

$$F = \frac{c - (s + \frac{l_2 - l_3}{l_1}) g(\alpha, \mu)}{c - (s + \frac{l_2 - l_3}{l_1}) g(0, \mu)} \cdot \frac{c - (s + \frac{3}{2}k) g(0, \mu)}{c - (s + \frac{3}{2}k) g(\alpha, \mu)} \tag{22}$$

where

$$g(\alpha, \mu) = \frac{-\mu + \tan\alpha}{\mu \tan\alpha + 1} \tag{23}$$

For $l_2 = l_3 = 0$, of course, $F = 1$, as expected from the result of the case study:part1. By using eq.(22), we can further find a couple of interesting properties. For simplicity, we assume $l_2 = l_3$ and $\beta = 0$, which makes the sensor configuration as shown in Fig.3(b). With this assumption, eq.(22) results in

$$F = \frac{1 - \frac{3}{2}k g(0, \mu)}{1 - \frac{3}{2}k g(\alpha, \mu)} \tag{24}$$

$$= \frac{1 + \frac{3}{2}k\mu}{1 + \frac{3}{2}k h(\alpha, \mu)} \tag{25}$$

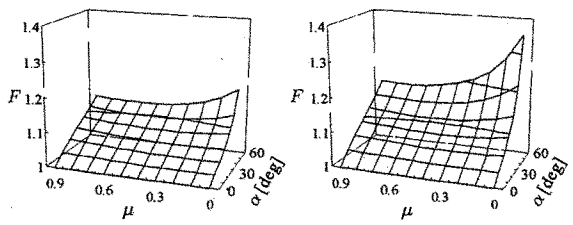


(a) $l_2/l_1$=0.033 (b) $l_2/l_1$=0.117

**Fig. 4**: Simulation

where

$$h(\alpha, \mu) = \frac{1}{\tan\alpha} - \frac{\tan\alpha + \frac{1}{\tan\alpha}}{\mu\tan\alpha + 1} \tag{26}$$

Now, suppose $\mu = 0$ for further simplicity. Under such a condition, eq.(24) reduces to

$$F = \frac{1}{1 - \frac{3}{2}k\tan\alpha} \tag{27}$$

$F > 1$ is guaranteed for $0 < \alpha < \alpha_1$, where $\alpha_1 = \tan^{-1}(2/3k)$. As pointed out in 3.4, for the surface with the inclination angle of $\alpha_1$, the contact force cannot make any displacement in the $y$-direction at the tip of whisker. For a whisker shape satisfying $l_2 \ll l_1$ ($k \ll 1$), however $\alpha_1$ should be close to $\pi/2$. Therefore, we can exclude such a singular angle from the practical range of $\alpha$, since $\alpha$ is at most $\pi/3$ for the slope given by dies. The edge enhancement effect, of course, appears under frictional contact ($\mu \neq 0$), while the discussion above is given under $\mu = 0$. Thus, the $L$-shaped whisker as shown in Fig.3(b) can work as a Tactile Differentiator, while the degree of amplification depends upon contact friction and the inclination angle.

### 3.7 Simulation

Fig.4 shows the basic behavior of $F$ for the $L$-shaped whisker under $\beta = 0$, where Fig.4(a) and (b) are computed for $l_2/l_1 = 0.033$ and $l_2/l_1 = 0.117$, respectively. These parameters for $l_2/l_1$ are same as those used in experiments. From both results, we can see that the edge enhancement effect becomes dominant as $\alpha$ increases. This implies that the effect is enhanced under a large intersection angle. We would note that the effect appears even under frictionless contact. Since the friction between whisker tip and metal surface is generally in order between 0.1 and 0.5, this result guarantees that we can easily see the edge enhancement in experiments.

## 4 Experiments

### 4.1 Experimental System

Fig.5 shows the experimental system with an $L$-shaped whisker where (a), (b) and (c) are an overview of the system, the sensing part, and an example of test piece ($\alpha = \pi/3$), respectively. The sensing part can be moved up-and-down by a DC servo-motor installed at the top of the system. A strain gauge is attached at the sensor base so that we can measure the moment caused by the contact force at the tip of whisker. The intersection angle produced by dies is roughly between $\pi/6$ and $\pi/3$. Considering this fact, we prepared three kinds of test samples where $\alpha = \pi/6$, $\pi/4$ and $\pi/3$, respectively. For simplicity, $\beta$ is fixed to zero, and $\alpha$ and $l_2/l_1$ are changed depending upon experiments.

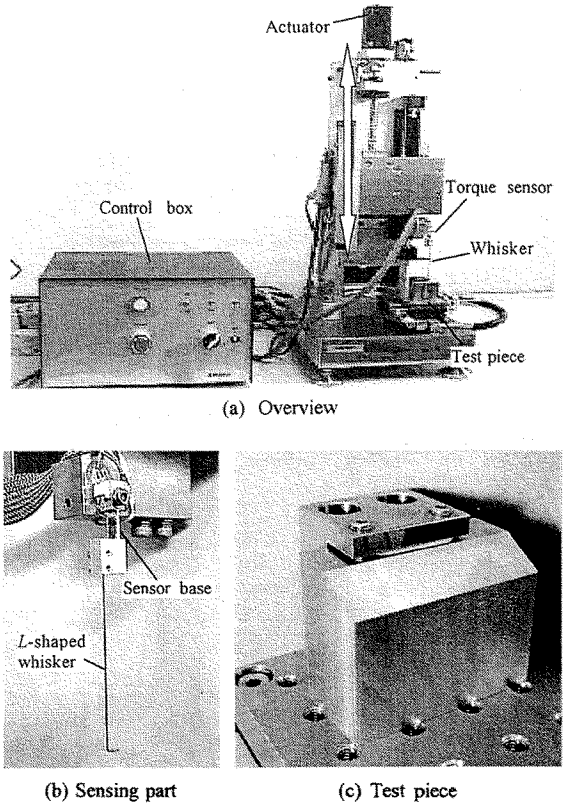


(a) Overview

(b) Sensing part (c) Test piece

**Fig. 5**: Experimental system

### 4.2 Experimental Results

(a)$l_2/l_1 = 0.083$: Under $\beta = 0$, the edge enhancement factor $F$ results in an extremely simple form, as shown in eq.(24) and is controlled by three parameters $l_2/l_1$, $\mu$ and $\alpha$. Therefore, we can consider the experimental results without much effort on parameter survey. Fig.6 shows the experimental results for three different test surfaces under $l_2/l_1 = 0.083$ where $\alpha = \pi/6$, $\pi/4$ and $\pi/3$, respectively. From Fig.6, we can clearly observe the edge enhancement effect for both $\alpha = \pi/4$ and $\pi/3$ and it is amplified for a lager $\alpha$.

(b)$\alpha = \pi/3$: Under $\alpha = \pi/3$, Fig.7 shows the experimental results for three different whiskers where (a), (b), (c) and (d) are $l_2/l_1 = 0.0$, 0.033, 0.083, and 0.117, respectively. The edge enhancement effect is still observed for different length of whisker, while the amplification varies according to the length.

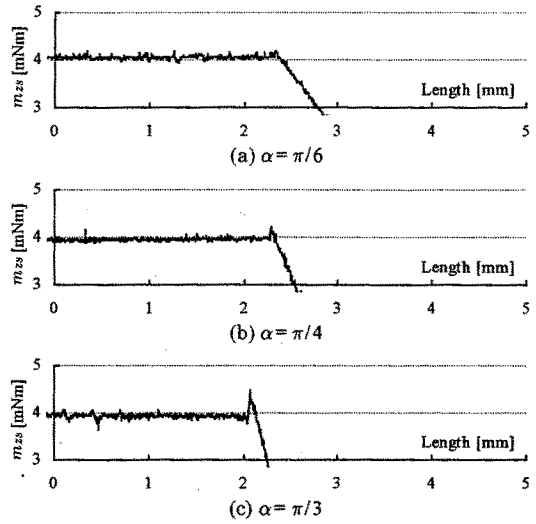


**Fig. 6**: Experimental results ($l_2/l_1 = 0.083$)

Through these experiments, we can clearly observe the edge enhancement effect. We believe that such sensor signals will be really effective when judging where the edge is. Because we can directly obtain the edge enhanced signal without any filtering process.

## 5 Concluding Remarks

We proposed the Tactile Differentiator which can enhance the edge where the whisker passes. As an important measure for evaluating the signal jump just before and after passing over an edge, the edge enhancement factor was introduced. We showed that a simple whisker with $L$-shape can work as a nice Tactile Differentiator through experiments. For recognizing the mark given by dies, more than one probing are necessary and this might be equivalently achieved by mounting plural number of whiskers at the sensor base. Since $F$ varies according to whisker shape, we can also design a Tactile Differentiator sensitive for particular inclination angle. The authors would express our sincere thanks for Mr. Akihiko Mizuno and Mr. Toshihiko Sajima for their helps for preparing this paper. The authors are also thankful for MITUTOYO Co. for providing us with the experimental system.

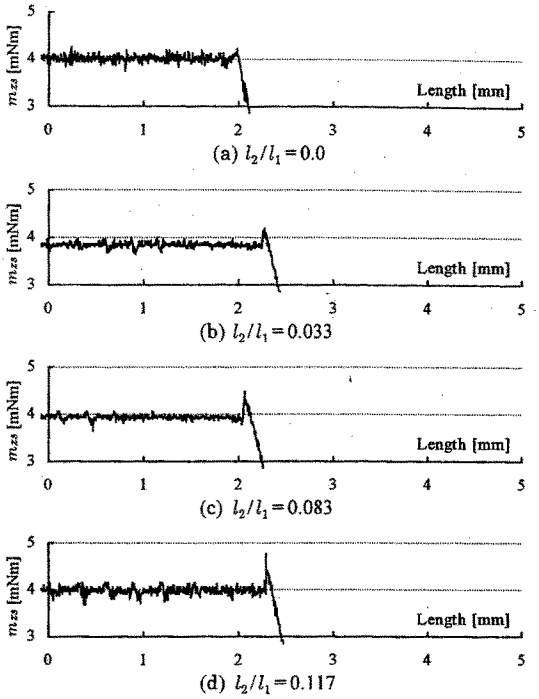


**Fig. 7**: Experimental results ($\alpha = \pi/3$)

## References

[1] M. Shimojo, M. Shinohara, and Y. Fukui: Human Shape Recognition Performance for 3-D Tactile Display, *IEEE Trans. on Systems, Man, and Cybernetics*, Part A, vol. 29, No. 6, pp.637-644, November 1999

[2] J. S. Son and R. D. Howe: Tactile Sensing and Stiffness Control with Multifingered Hands, *Proc. of the 1996 IEEE Int. Conf. Robotics and Automation*, vol. 4, pp.3228–3233, 1996

[3] H. Maekawa, K. Tanie, K. Komoriya, and M. Kaneko: Development of a Finger-Shaped Tactile Sensor and its Evaluation by Active Touch, *Proc. of the 1992 IEEE Int. Conf. Robotics and Automation*, vol. 2, pp.1327–1334, 1992

[4] M. Ueda, et al.: Tactile Sensors for Industrial Robot to Detect Slip, *Proc. of the 2nd ISIR*, IIT Research Institute, Chicago, pp.63–76, 1972

[5] R. D. Howe and M. R. Cutkosky: Sensing skin acceleration for slip and texture perception, *Proc. of the 1989 IEEE Int. Conf. Robotics and Automation*, pp. 145-150. 1989

[6] R. D. Howe and M. R. Cutkosky: Touch Sensing for Robotic Manipulation and Recognition, *The Robotics Review 2, O. Khatib, et al., eds.*, MIT Press, pp. 55-112, 1992

[7] R. A. Russel: Closing the sensor-computer-robot control loop, *Robot Age*, pp.15–20, Apr. 1984

[8] S. S. M. Wang and P. M. Will: Sensors for computer controlled mechanical assembly, *Ind. Robot*, pp. 9–18, Mar. 1978

[9] P. McKerrow: *Introduction to Robotics*. Reading, MA: Addison Wesley, 1990

[10] R. A. Brooks: A robot that walks; Emergent behaviors from a carefully evolved network, *Neural Computat.*, vol. 1, pp. 253–262, 1989

[11] S. Hirose *et al.*: Titan III, A quadruped walking vehicle, *Proc. 2nd Int. Symp. Robot Res.*, Cambridge, MA, 1985

[12] R. A. Russel: Using tactile whiskers to measure surface contours, *Proc. of the 1992 IEEE Int. Conf. on Robotics and Automation*, pp. 1295–1300, 1992

[13] M. Kaneko and T. Tsuji: A Whisker Tracing Sensor with 5$\mu$m Sensitivity, *Proc. of the 2000 IEEE Int. Conf. on Robotics and Automation*, pp. 3907–3912, 2000